



## RESEARCH ARTICLE

### PETROLOGY, GEOCHEMISTRY AND TECTONIC ENVIRONMENT OF IGNEOUS COMPLEX IN THE NEOPROTEROZOIC MAYO KEBBI BASIN, CHAD

**Leontine Tekoum<sup>1,2</sup>, Doumnang Mbai gane J.C<sup>1</sup>, E. Kadjangaba<sup>3</sup>, Ye Qian<sup>2</sup>, Da Wang Guang<sup>2</sup> and Fengyue Sun<sup>2</sup>**

<sup>1</sup>Laboratoire de Géologie, Géomorphologie et Télédétection, Département de Géologie, Faculté des Sciences Exactes et Appliquées, Université de N'Djaména; <sup>2</sup>College of Earth Sciences, Jilin University, Changchun, Jilin 130061, People's Republic of China; <sup>3</sup>Geology Department, Faculty of Science and Technology, University of Doba, rue de Gaki, Chad

#### ARTICLE INFO

##### Article History:

Received 16<sup>th</sup> October, 2022

Received in revised form

19<sup>th</sup> November, 2022

Accepted 15<sup>th</sup> December, 2022

Published online 20<sup>th</sup> January, 2023

##### Key words:

LA-ICP-MS Zircon U-Pb dating;  
Geochemistry; Geodynamic; Igneous intrusion; Neoproterozoic, Mayo kebbi Southwestern Chad.

##### \*Corresponding Author:

Leontine Tekoum

#### ABSTRACT

The Mayo kebbi mafic-ultramafic intrusions are represented by gneiss–amphibolite complex, which is exposed east of the Zalbi Group. They consist mainly of gabbro-diorite, amphibolites, gneiss amphibole, hornblende and pyroxenite. The mineral assemblages are characterised by amphibole (hornblende), plagioclase, pyroxene and chlorite. Our electron microprobe analysis showed that, the most of mafic –ultramafic rock mineral are calcic-amphibole. Where hornblende are more Magnesio ( $Fe^{2+} < Mg$ ) than ferro-hornblende, this is may be due to the lack of the hydrothermal alteration of clinopyroxene. Cathodoluminescence image of zircon from the amphibolites reveal magmatic oscillatory zoning with inherited cores and high ratio U/Th (0.14 - 1.75), imply their magmatic origin. The LA-ICP-MS zircon U-Pb isotopic Concordia diagram yield an age of  $692 \pm 11$  Ma (MSWD = 1.3),  $718.4 \pm 8.2$  Ma (MSWD=0.46),  $691 \pm 4.7$  Ma (MSWD = 0.43) and  $800.7 \pm 6.7$  Ma (MSWD=0.46). We can interpret as the emplacement age of the gabbro in Mayo Kebbi area. The igneous complexes were derived from a juvenile Neoproterozoic source. Geochemistry and tectonic setting indicated that the amphibolites rocks from Mayo kebbi are derived from volcanic arc basalt. Tectonic discrimination diagrams using chemical attributes suggest a tholeiitic to calc-alkaline affinity for the mafic intrusive and probably formed in back arc setting. All of these rocks have very low rare earth element fractionation ((La/Yb) N= 0.41 to 1.68). They are depleted in LREE which are derived from same parental magmas.

Copyright©2023, Leontine Tekoum et al. This is an open access article distributed under the Creative Commons Attribution License, which permits unrestricted use, distribution, and reproduction in any medium, provided the original work is properly cited.

Citation: Leontine Tekoum, Doumnang Mbai gane J.C, E. Kadjangaba, Ye Qian et al. 2023. "Petrology, Geochemistry and Tectonic environment of Igneous complex in the Neoproterozoic Mayo Kebbi Basin, CHAD". *International Journal of Current Research*, 15, (01), 23253-23260.

## INTRODUCTION

Situated in the border part of the heterogenous Saharan metacraton Abdelsalam et al. (2002), the Mayo Kebbi orogenic belt is one of an important metallogenic belt in Chad. According to Abdelsalam et al. (2002), the Saharan Metacraton is essentially Archaean and Palaeoproterozoic continental crusts that has been overprinted by Neoproterozoic tectono-metamorphic events and also contains Neoproterozoic juvenile material. Many economic deposits are founded along southern margin: gold, uranium, copper, chromium, nickel and platinum Index. The exposed part of this terrane is made up by metavolcanics and metasedimentary intruded by late-to post-tectonic granites and diorites most of which have different radiometric age (Doumnang et al., 2004 and Penaye et al., 2006). The Mayo kebbi igneous complex is poorly surveyed, particularly regard to geochronological and geochemical studies. The mafic to intermediate complex correspond to G1 Group which is characterized by compressional deformation and shearing.

It consists of protomylonitic to mylonitic kilometre-scale intrusions of gabbroic to dioritic rocks located at the borders of the Zalbi Basin (Penaye et al., 2006). This complex also includes meta-plutonic rocks consisting dominantly of metadiorites that are associated with minor gabbros, norites, and peridotites. Kasser (1995) used the term “mafic to intermediate complex” as equivalent of the gneiss–amphibolite complex of Schneider and Wolff (1992). All these rock units are intruded by post-tectonic granitoids (Penaye et al., 2006). The gneiss–amphibolite complex as defined by Schneider and Wolff (1992) is exposed east of the Zalbi Group and also found as numerous xenoliths within the tonalite batholith. This complex comprises hornblende-biotite gneisses interlayered with banded amphibolites; the presence of calc-silicate layers associated with amphibolite suggests that part of this unit is of sedimentary origin (Penaye et al., 2006). In the present study, except the field observations, geochronological and geochemical data of the igneous rocks in the Mayo Kebbi region, Southwestern Chad need to be addressed in order to understand their significance and discuss their tectonic setting in the Pan-African orogens.

**Regional geology:** The Mayo Kebbi massif south west Chad is situated in the border part of the Saharan metacraton that lies between the Congo craton in the south and the Nigerian Shield in the west (Liégeois, J.P et al., 2012). (Fig.1). A series of uplifted areas within the Saharan metacraton including Mayo Kebbi, Chad Massif Central, Waddai, Darfur to Bayuda (Fig. 1) display similar characteristics: (1) the presence of metamorphic Palaeoproterozoic and Archean protoliths (Adamawa-Yade block in Mayo Kebbi; Penaye et al., 2006; Pouclet et al., 2006), (2) the presence of overthrust island arc lithologies towards the Saharan metacraton (Pouclet et al., 2006) and (3) the presence of Neoproterozoic high-K calc-alkaline batholiths mainly of crustal origin (Liégeois, J.P et al., 2012). The Mayo Kebbi massif is described as a juvenile Neoproterozoic crust (Penaye et al., 2006; Pouclet et al., 2006) which belongs, together with the Yade massif, to the Central African Orogenic Belt (CAOB) (Isseini, M et al., 2012). The magmatic rocks outcropping in the Mayo Kebbi massif have been recently interpreted as resulting from Neoproterozoic juvenile accretion in an arc setting (Kasser, 1995; Pouclet et al., 2006). This terrane represents an active margin system that was accreted onto the Adamaua-Yade continental block along the Tchollire tectonic zone during the WNW-ESE compressional event (Penaye et al., 2006). The Mayo Kebbi batholith consists of a variety of more or less deformed rocks types. The various lithologies are dominant by green rock (Zalbi Serie), biotite granite, oriented granite, quartz dioritic, pyroxenite, gneiss amphibolite (Figure 2). The mafic-ultramafic body is a Neoproterozoic intrusion, as indicated by the most recent geochronological data  $777 \pm 5$  (zircon U-Pb; Doumnang 2006).

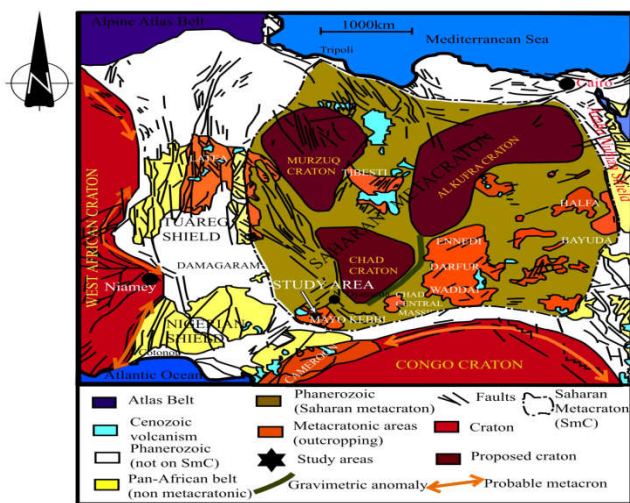


**Fig. 1. Main rheological domain of Saharan Africa centered on the Saharan metacraton Showing the study areas (After Liégeois, J.-P., et al., 2012 (Milesi et al., 2010), Fezaa et al. (2010), Küster et al. (2008), (Cratchley et al., 1984)**

**Petrography:** Based on the petrographical observations, the amphibolites of the study area exhibit fine-medium and medium coarse-grained massive or porphyry texture. The rock contain mainly pyroxenes, amphibole (hornblende), feldspars (plagioclase and K-feldspars), biotite, epidote, actinolite, magnetite and quartz. Plagioclase up to 2mm in size is the most abundant phenocryst phase in the all samples of mafic ultramafic intrusive rocks. They are generally euhedral to lath shape. The presence of feldspar in the rock samples are well matched with positive Eu anomaly in the REE pattern. Massive amphibolites coarse -grained massive (Fig.3. a) or porphyry texture and mainly contain plagioclase (35-40 vol %) hornblende (40-45 vol %) biotite (5-15 vol %) and quartz (5 vol %) these biotites are altered to chlorite and epidote. Accessory minerals include epidote, zircon, anatite, pyrite and magnetite. Hornblende occurs in the locality as transparent euhedral to subehedral phenocryst. Pyroxenes are most abundant phenocryst in some samples sometimes altered to hornblende and actinolite. The intrusive contains minor interstitial quartz, which has a round shape (Fig.3. B).

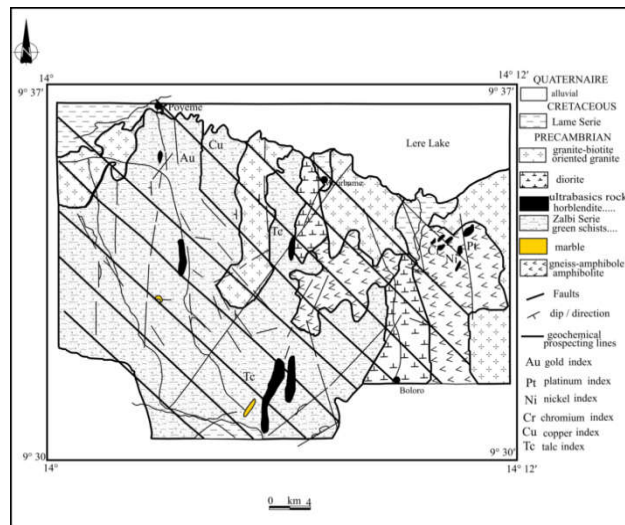


**Fig.2. Geological and mineral resources map of the Mourbamé Sector, South Léré Lake (After Courtesy A. Beauvilain 1995 CNAR)**

Accessory minerals include epidote, zircon, apatite, pyrite and magnetite. Ilmenite, magnetite and titanomagnetit appear as opaque minerals. The rock samples have a porphyritic texture with large euhedral clinopyroxene and rare plagioclase phenocrysts set in a fine-grained groundmass made up of euhedral plagioclase, amphibole, quartz and K-feldspar (Fig. 3 c). In addition, plagioclase phenocrysts are generally well preserved throughout the hole; they often are totally transformed into pseudomorphic chlorite aggregates. In other cases, pyroxene is almost completely replaced by actinolite, starting from the rims, but occasionally leaving intact little pyroxene portions in which the typical high interference colors are preserved (Fig. 3 d). In the hand specimen layered amphibolites show fine texture and mainly contain: hornblende (50-55 vol %), plagioclase (25-30 vol %) chlorite (5-15 vol %) and oxides. Accessory minerals include epidote, zircon, apatite, and magnetite (Fig. 3 e).

The pyroxenite rock samples have a porphyritic texture with large euhedral clinopyroxene and rare plagioclase phenocrysts set in a fine-grained groundmass made up of euhedral plagioclase, amphibole, quartz and K-feldspar (Fig.4 a.b). In addition, plagioclase phenocrysts are generally well preserved throughout the hole; they often are totally transformed into pseudomorphic chlorite aggregates. In other cases, pyroxene is almost completely replaced by actinolite, starting from the rims, but occasionally leaving intact little pyroxene portions in which the typically high interference colors are preserved (Fig.4.c). Hornblende rocks have fault texture and shows granular crystalline of hornblende (85-90%), epidote (3-5%) and relic pyroxenes (3-5%) (Fig.4.e).

**Electron micro probe analysis:** The electron probe analysis was done by Japan Electronics (JEOL) JXA-8230 electron probe micro-analyzer in the Bureau of China Metallurgical Geology, Shandong Test Center.

The Analytical conditions are operating voltage: 20kV sulfur oxides 15KV with Current of 20nA and analysis of the beam spot is 1um-5um. Integration time of major elements (content greater than 1%) peak integration time is 10s and background integration time 5s. Microelements peak integration time is 20s, background integration time 10s. Standard sample selection and test ideas:

American SPI standard sample selection criteria and metallic mineral standards, standard test conditions consistent with the unknown samples, to ensure the stability of standard samples were tested for each standard five point standard test count rate stable and reliable.

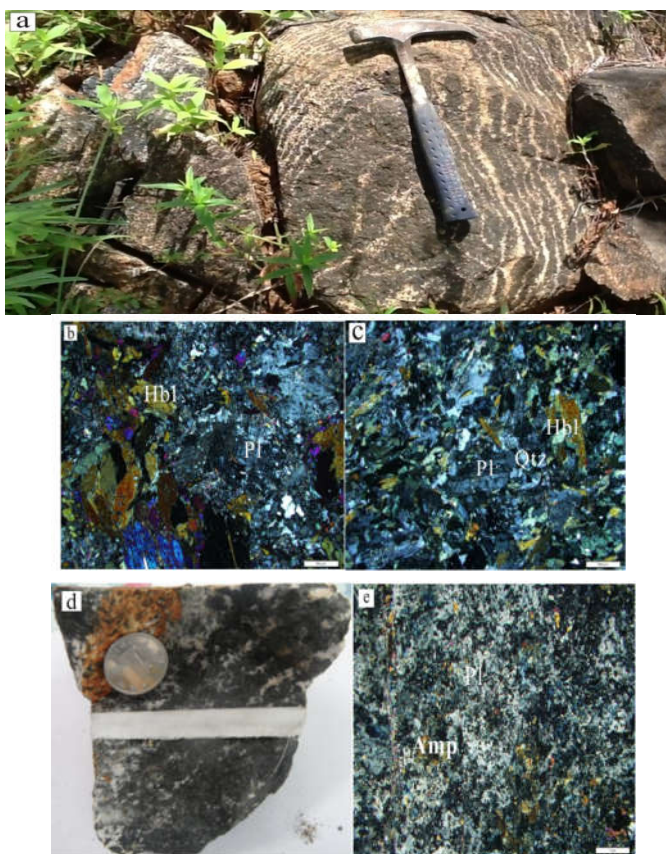


**Fig. 3.** Photograph of Doue South Léré Lake (a) massive banded amphibolite, (d) gneissic amphibolite (b), (c) polarized photomicrograph of massive amphibolites, (e) polarized photomicrograph of gneiss amphibole showing Hbl: hornblende, Pl: plagioclase Amp: amphibole and Qtz: quartz

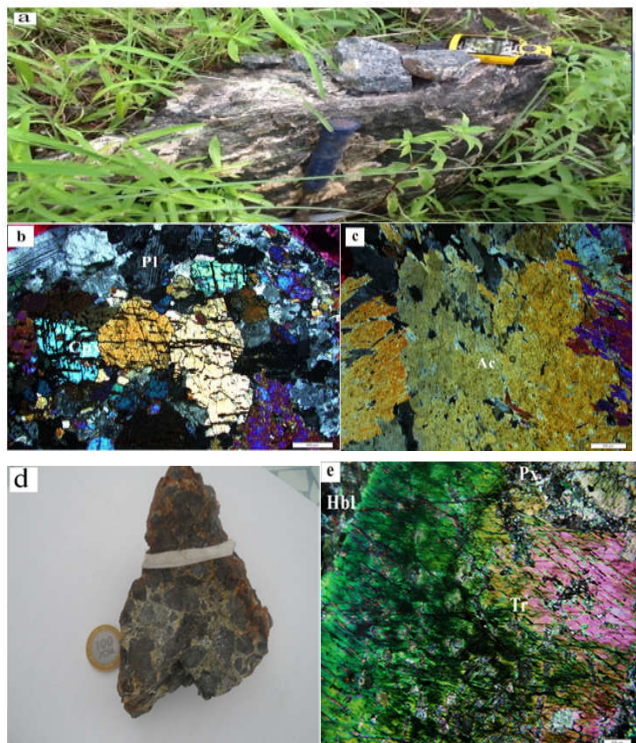


**Fig. 4.** FieldPhotograph of Doue South Léré Lake (a) massive pyroxene - amphibolite, (d) euheral to subhedral hornblende xenocrysts in amphibolite (b), (c) polarized photo micrograph of massive pyroxene-amphibolites, (e): fault texture of amphibolites, showing : Hbl : hornblende, Tr : tremolite, pl : plagioclase, Qtz : quartz, Ac : Actinole, Cpx : Clinopyroxene

Our electron microprobe analysis showed that, the most of mafic – ultramafic rock mineral are calcic-amphobe. Where hornblende are more Magnesio ( $\text{Fe}^{2+} < \text{Mg}$ ) than ferro-hornblende, this is may be due to the lack of the hydrothermal alteration of clinopyroxene.

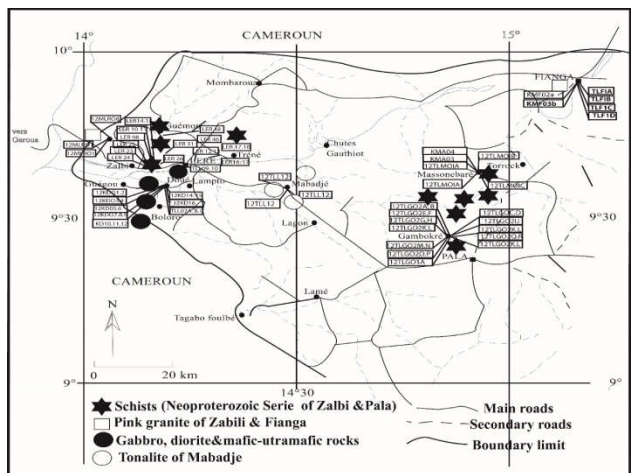


**Fig.5.** Map of sampling and outcropping

In clear contrast, secondary amphibole formed at the expense of clinopyroxene of mafic ultramafic rock is mostly tremolite, actinolite (Fig.6.)

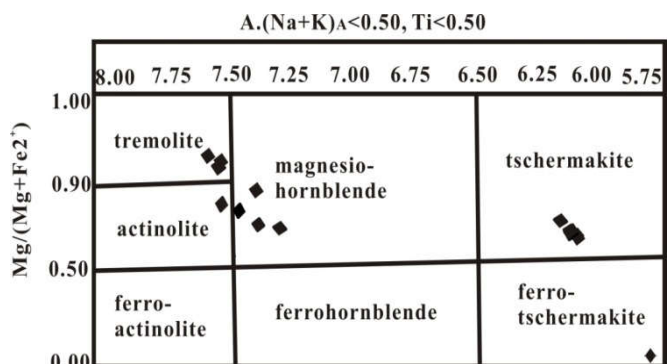


**Fig.6:** Compositional ranges of magma Ca-amphiboles from the mafic ultramafic rocks of Mayo Kebbi expressed in the classification diagram of Leake et al. (1997)

**Analytic methods :** For geochemical analysis of the study, 9 samples for ultramafic-mafic intrusions from south Léré Lake and 8 granitoid samples from Fianga Teubang and Zabili were analyzed for major elements oxides using the standard X-ray Fluorescence (XRF) techniques and trace elements by an inductively-coupled plasma-mass spectrometer LA-ICP-MS at the Guangzhou City, Guangdong Province ALS Laboratory Group of American Industrial Estate. Major and trace elements analysis are presented in the table 1 and 2. Selected Major and trace elements (Ba, Rb, Sr, Cr, Sc, V, Zn, and Zr) were determined by wavelength-dispersive XRF on pressed powder pellets. Cs, Ga, Nb, Pb, Ta, Th, U, Y and the rare earth elements (Ce, Dy, Er, Eu, Gd, Ho, Lu, Nd, Pr, Sc, Sm, Tb, Yb) were analyzed by ICP-MS, on solutions obtained by HF dissolution of fused glass disks. The multi-element analyses for Mayo Kebbi gold were determined by ICP-MS on solutions obtained by HF dissolution of fused glass disks. The wall rock samples from Mayo Kebbi were first prepared (crushing and milling) at Earth Science College, Jilin University, Changchun, China. Major and trace element analyses of the wall rock samples were then performed at Testing Center of Jilin University, Changchun, China. Both major and trace element samples were prepared using LiBO<sub>2</sub> fusion. Major elements were then analysed by ICP-ES, and for the trace element analysis ICP-MS was used. Each sample was also separately analyzed for gold by fire assay fusion and ICP-ES.

The LA-ICP-MS dating samples were collected from amphibolite using heavy liquid and magnetic separation techniques. The zircons were analyzed by LA-ICP-MS at Northwest University (China), Department of Geology, State Key Laboratory of Continental Dynamics. The laser ablation system is a ComPex102 equipped with a (wavelength 193 nm) ArF-excimer laser and Analyses were performed with a dynamic reaction cell ICP-MS, quadripolar Elan6100DRC type. Cathodoluminescence (CL) images of zircons were prepared prior to analysis in order to characterize internal structure and to target potential site for U-Pb dating. U-Pb isotopic ratios were calculated using the Glitter software (ver. 4.0 Macquarie University) (Andersen, 2002). The U-Pb age calculation and concordia plot were obtained using the ISOPLOT software program (Ludwig, 2003).

## Analysis result

### Geochemical result

**Major oxides:** Nine rock samples of Mayo Kebbi ultramafic to mafic intrusion were selected for geochemical analysis. The Major oxide composition of the samples is characterized by low to moderate  $\text{Al}_2\text{O}_3$  7.07% - 17.38%. In the Hornblende- Pyroxenite, the  $\text{SiO}_2$  content ranges from 44.5% to 51.37% and that of  $\text{TiO}_2$  is fairly low and range from 0.65% to 0.83%. The high content of  $\text{MgO}$  12.17%-14.62% can probably indicate olivine or pyroxene (clinopyroxene) accumulation. They have relatively higher  $\text{CaO}$  13.76%-14.99% content and it may be result to garnet like a residual phase in the mantle, characteristic of ultramafic rocks.

The lower  $\text{Na}_2\text{O}+\text{K}_2\text{O}$  0.93%-1.69% and the  $\text{Na}_2\text{O}$  content are high than  $\text{K}_2\text{O}$  indicating that Na is more enriched than K. In the amphibolites, the  $\text{SiO}_2$  content ranges from 47.27% to 47.99% and that of  $\text{TiO}_2$  from 1.3% -1.45% and have significantly lower  $\text{MgO}$  4.99%-6.39 %. In addition, the lower  $\text{Na}_2\text{O}+\text{K}_2\text{O}$  ranging from 2.49% to 3.06% and the  $\text{Na}_2\text{O}$  content are much higher than  $\text{K}_2\text{O}$  indicating that Na are also more enriched than K. **The low alkali contents are typical** of tholeitic series (Schilling et al., 1983, Sun and McDonough, 1989). On the AFM ternary diagram with the dividing lines of Irvine & Baragar (1971) to discriminate between tholeitic and calc-alkaline suites, the samples plot all in the high tholeitic trend (Fig. 7. a) suggesting that, the mafic-ultramafic rocks were crystallized from similar parent magma. In the ternary discrimination diagrams of (Pearce et al., 1977) the samples plot in the continental basalt field, some plot into the OIB and MORB field probably due to their cumulate effects (Fig.7. b).

In the ternary discrimination diagrams of (Pearce et al. 1977) the samples plot in the Island- Arc Tholeite (IAT) field (Fig.7. c). On the  $\text{Zr}/\text{TiO}_2$  vs.  $\text{Nb}/\text{Y}$  classification diagram of (Winchester and Floyd 1976), all samples plot in sub-alkaline basalt field with ( $\text{Nb}/\text{Y} < 0.07$ ) (Fig. 7. d). These rocks have a loss on ignition (LOI) values from 1.24 to 2.89 wt. % (Table 2) suggesting probably the contribution of secondary hydrated and carbonate phases. According to the total alkali vs. silica (TAS) discrimination diagrams of (le Bas et al., 1986) all rocks plot in gabbro (basalt) field(Fig.7.e). All these characteristics of hornblendites and homblende pyroxenite in Mayo kebbi area are similar to those of the ultramafic rocks of the Pan African complex Mokuru in Ilesha schist belt, south-eastern Nigeria (Ige et al., 1998).

### Rare earth elements

Chondrite-normalized REE patterns of amphibolites presented give little precision in the differentiation process of fractional mineral, because the distribution is nearly flat with no or weak positive Eu anomalies ( $\delta\text{Eu}$  ranges from 0.86 to 1.18) and show slightly LREE-depleted type (Fig.8.a). ( $(\text{La}/\text{Yb})_N = 0.41$  to 1.40). The total REEs content of Px-amphibolites is lower, varying from (14.98-35.62) and weak LREE/HREE fractionation (1.65—2.0) with ( $\delta\text{Ce}$  ranges from 0.91 to 1.00).

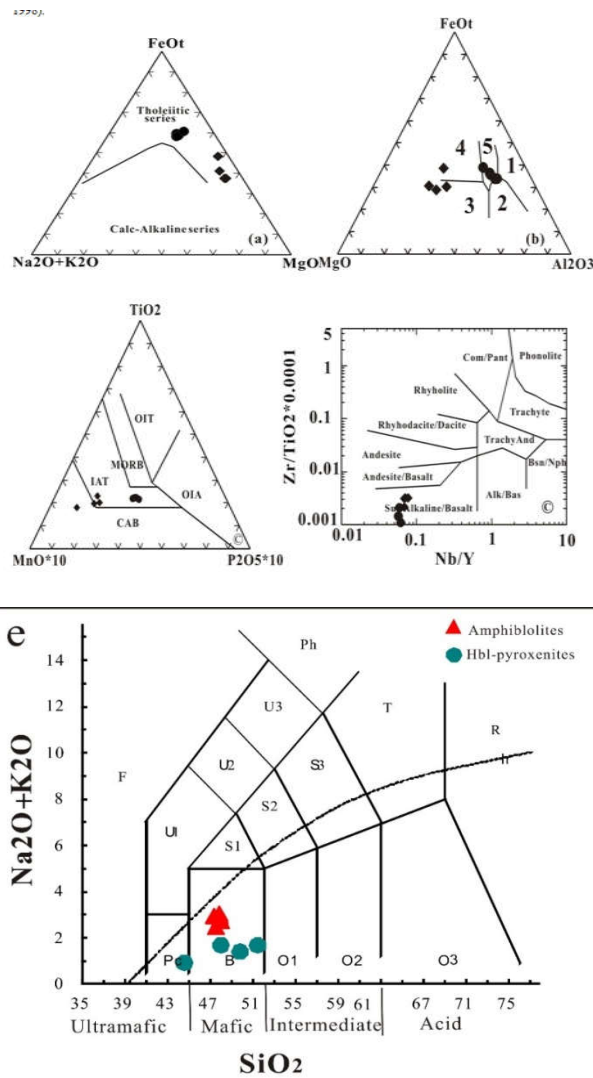


**Fig. 7.** Diagram for mafic-ultramafic rocks from south Léré Lake Mayo Kebbi, (a) AFM diagram modified after Irvine and Barager (1971). (b) Ternary discrimination diagrams modified after Pearce et al. (1977). 1 SC, spreading center island; 2 IA, island arc; CM, continental margin; 3, MORB, Mid-ocean Ridge Basalt 4 OIB, oceanic island basalts; 5 CB, continental basalts (c) Ternary discrimination diagrams modified after Mullen (1983) fields are Oceanic-Island Tholeiite (OIT); Mid-ocean Ridge Basalt (MORB); Island- Arc Tholeiite (IAT); Ocean Island Alkali Basalt and Calc-Alkaline Basalt (CAB). (d)  $\text{Zr}/\text{TiO}_2 \times 0.0001$ - $\text{Nb}/\text{Y}$  diagram after Winchester and Floyd (1976). (e) Mafic ultramafic rocks from (Lere) in Chad plotted in the Total-Alkali Silica (TAS) diagram of (Le Bas et al., 1986), P = picro basalt, B = basalt, O1 = basalt andesite, O2 = andesite, O3 = dacite, R = rhyolite, S1 = trachybasalt, S2 = basaltic trachyandesite, S3 = trachyandesite, T= trachyte and trachydacite, U1 = terphrite and basanite, U2 = phonotephrite, U3 = tephriphonolite, Ph = phonolite, F = foidite

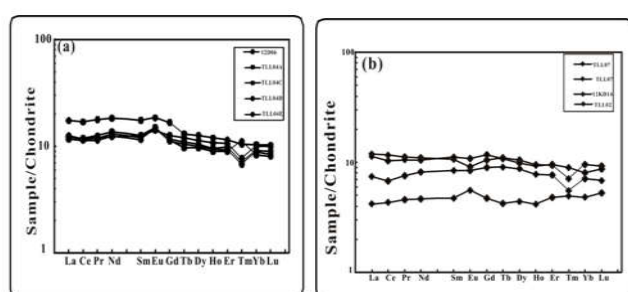


**Fig. 8. (a) and (b)** Chondrite-normalised REE patterns for mafic ultramafic rocks from south Léré Lake (Chondrite Normalized values are from Boynton 1984)

Chondrite-normalized REE patterns of Hornblende-pyroxenite have pronounced negative Tm anomaly and positive Eu anomaly with ( $\delta\text{Eu}$ ) ranges from 1.08 to 1.28) show slightly LREE-depleted type (Fig.8. b) ( $(\text{La/Yb})_{\text{N}} = 1.23 - 1.68$ ). The total REEs content of Hbl - amphibolite is lower, varying from 36.60 to 52.19 with similar ranges of composition of LREE/HREE ratio (2.02— 2.45), and ( $\delta\text{Ce}$ ) ranges from 0.96 to 0.99). The positive Eu-anomaly is usually interpreted as result of the early plagioclase accumulation in the magma chamber. These rock shows flat and slight pattern, suggesting that they are probably derived from a depleted mantle source (Pearce, 1980). All of these rocks have very low rare earth element fractionation ( $(\text{La/Yb})_{\text{N}} = 0.41$  to 1.68). Tectonic setting discrimination: In this study, the tectonic setting where the Mayo Kebbi Group formed is debated. The geochemical signature of tholeiitic metavolcanic rocks suggests their **development in an island-arc and back-arc setting** (Kasser, 1995; Doumnang et al., 2004). The tectonic setting discrimination diagrams are based upon multi-element variation among **different rock types** and formations of different environments. For the tectonic environment, Wood (1980) diagram based on the HFS elements is used to determine the types of amphibolites. Among samples from each of these diagrams (Th-Hf/3-Nb/16) and (Th- Zr/117-Nb/16), the first Hbl-amphibolite samples are in the island arc tholeiitic basalts and Hbl-pyroxenite cal-alkaline basalt field. In addition, all samples plot in the calc-alkaline basalts field, (Fig.9. (a) and (b)).

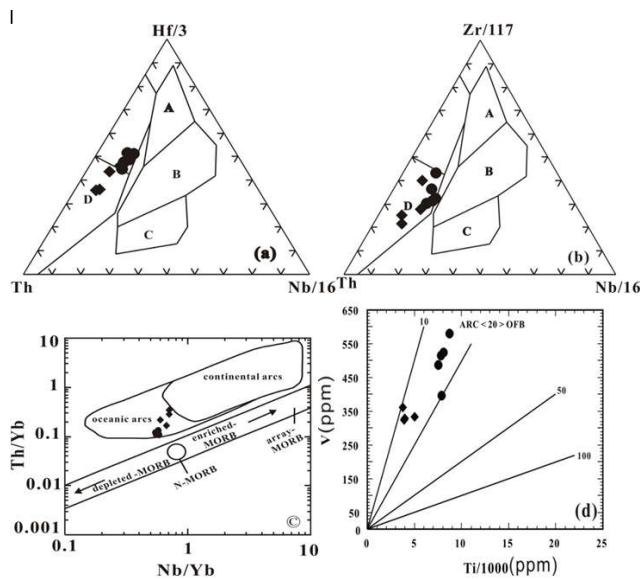


**Fig.9.** discrimination diagram of the Mayo kebbi igneous complex  
 (a) Hf/3-Th-Nb/16, and (b) Zr/117-Th-Nb/16 diagrams after Wood (1980). A: N-MORB: normal type mid-ocean ridge basalt; B: E-MORB: enriched type mid-ocean ridge basalt; C: WPB: within-plate basalt; D: SSZ supra-subduction zone, Back-arc and fore-arc basalts also plot within the SSZ field or IAT: island arc tholeiitic basalts and CAB: Cal-alkaline basalt. (C) Th/Yb vs. Nb/Yb diagram (after Pearce and Peate, 1995), (d) Ti/1000-V diagram after Shervais (1982). ARC: arc basalt; OFB: ocean floor basalt (MORB)

Based on those diagrams we can suggest that the Mayo Kebbi intrusion was formed in a continental margin. On the Th/Yb versus Nb/Yb variation diagram of Pearce and Peate (1995) the Neoproterozoic igneous rocks plot in the field of the oceanic arcs (Fig.9. (c)), this suggests that these rocks may be formed in an island arc environment rather than active continental margin.

They represent a partial melt of a depleted mantle source (N-MORB). On Ti/1000-V diagram of Shervais (1982), samples plot mainly within the island-arc tholeiite field, but one of the samples is transitional between island arc tholeiite and mid-ocean ridge basalt. The characteristic of tholeiitic rock (Fig.9. (d)) are consistent with the AFM diagram that shows trend of strongly tholeiitic suites.

## Description (Testing result)

### The ultramafic to mafic intrusions

**Pyroxenite:** Fifteen analyses of zircon from pyroxenite-hornblende rock were obtained for 12KD16 sample (Fig.10.a). Mass fraction of trace elements U and Th  $25.64 \times 10^{-6} \sim 1099.2 \times 10^{-6}$  and  $4.13 \times 10^{-6} \sim 60.156 \times 10^{-6}$  Th/U ratios (0.14 - 1.75), have geochemical characteristic of magmatic zircon. Measurement of zircons from the isotopic composition gave a weighted mean  $^{206}\text{Pb}/^{238}\text{U}$  age of  $800.7 \pm 6.7$  Ma (Fig.11a). Mean square weight deviation (MSWD=0.46) indicates the magmatic crystallization age of pyroxenite.

**Gneiss-amphibolites:** Ten analyses of zircon from the Gneiss-amphibolites sample (12KD11)(Fig.10.b)with mass fraction of trace element U and Th  $41.33 \times 10^{-6} \sim 216.26 \times 10^{-6}$  and  $15.02 \times 10^{-6} \sim 13.21 \times 10^{-6}$  Th/U ratios (0.3 - 0.62), have a weighted mean  $^{206}\text{Pb}/^{238}\text{U}$  age of  $692 \pm 11$  Ma (1). Mean square weight deviation (MSWD = 1.3) (Fig.11. b). This age can interpret to be the crystallization age of the Gneiss -amphibolites.

**Metagabbro:** Fifteen analyses of zircon from dominant Metagabbro rock were obtained for 12KD05 sample (Fig.10.c).Mass fraction of trace elements U and Th  $43.85 \times 10^{-6} \sim 148.32 \times 10^{-6}$  and  $15.59 \times 10^{-6} \sim 80.69 \times 10^{-6}$  Th / U ratios (0.29 - 0.61), have geochemical characteristic of magmatic zircon. Measurement of zircons from the isotopic composition gave a weighted mean  $^{206}\text{Pb}/^{238}\text{U}$  age of  $718.4 \pm 8.2$  Ma (Fig.11.c). Mean square weight deviation (MSWD=0.46)indicates the magmatic crystallization age of Metagabbro. We can interpret as the emplacement age of the Metagabbro in Mayo Kebbi area.

**Metadiorite:** Twelve analyses of zircon from Metadiorite sample (12KD07)with mass fraction of trace element U and Th  $36.86 \times 10^{-6} \sim 524.55 \times 10^{-6}$  and  $14.15 \times 10^{-6} \sim 431.36 \times 10^{-6}$  Th/U ratios (0.22– 0.82), have a weighted mean  $^{206}\text{Pb}/^{238}\text{U}$  age of  $691 \pm 4.7$  Ma (1). Mean square weight deviation (MSWD = 0.43)(Fig.11.d). This age can interpret to be the crystallization age of the Metadiorite.

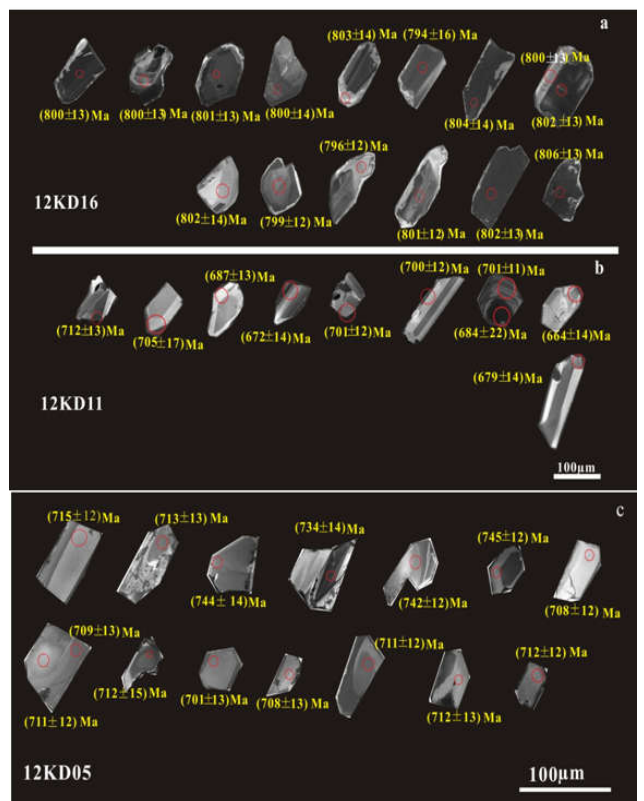


**Fig. 10.** Cathodoluminescence (CL) images of representative zircons of ultramafic to mafic intrusion from Mayo Kebbi

(a) Pyroxenite, (b) gneiss-amphibolites (c) metagabbro  
 Circle indicates the location of LA-MC-ICPMS

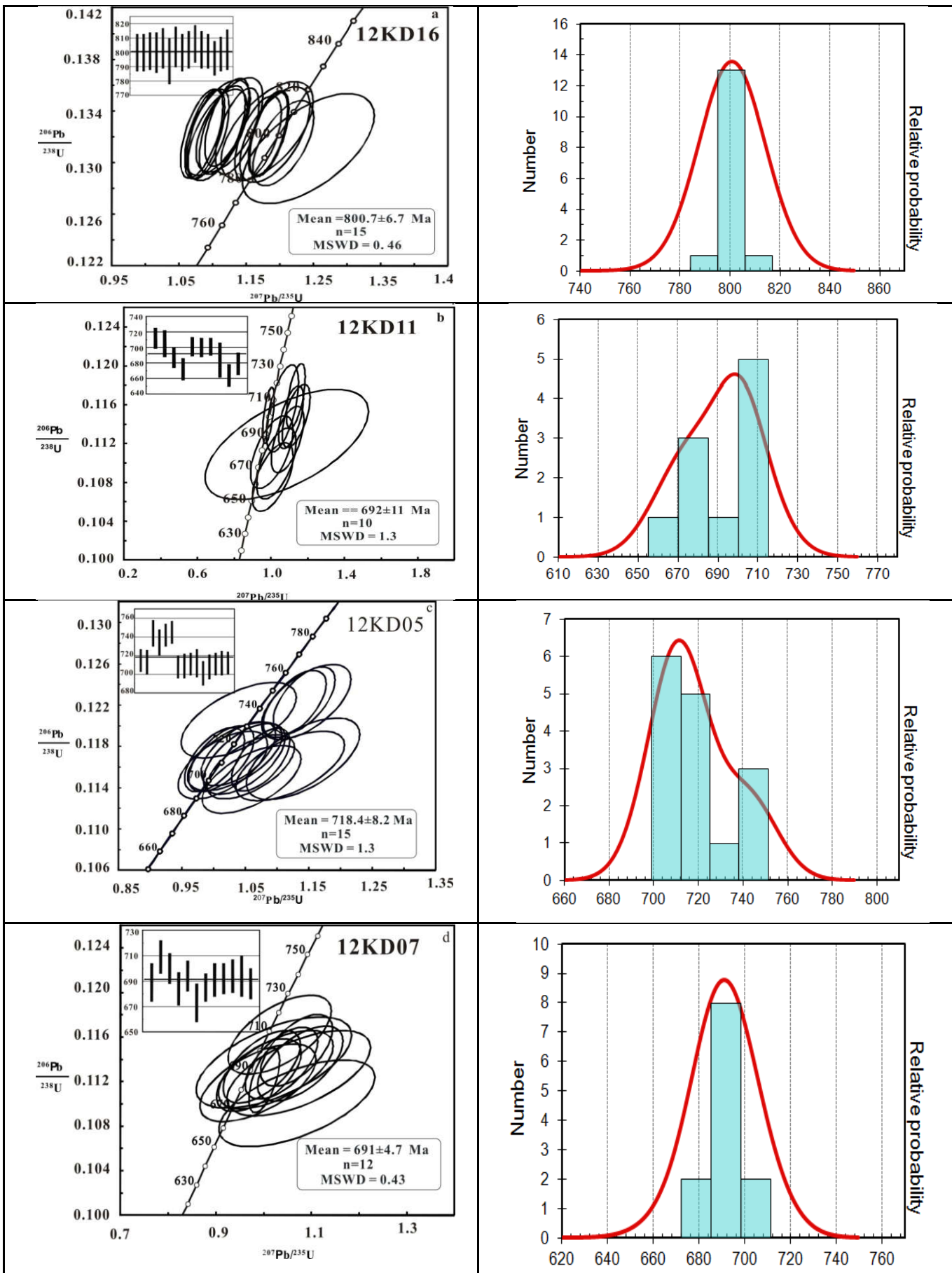


Fig.11. Concordia plot of LA-ICP-MS U-Pb data for zircons and their probability density of of ultramafic to mafic intrusion from Léré, Mayo Kebbi

## CONCLUSION AND DISCUSSION

In this paper, we present the new petrographical and geochemical data of neoproterozoic mafic-ultramafic intrusions from Mayo Kebbi. The mafic-ultramafic intrusions have preserved well their magmatic texture. The mineral assemblages are mainly characterised by amphibole (hornblende), plagioclase, pyroxene (clinopyroxene) and chlorite. Hornblende is present locally and has formed, probably, by replacement of pyroxene. These and other data point to major episodic igneous events during the Neoproterozoic for example in South China, Australia and many other parts of the Rodinia continent (Zhang *et al.*, 2009) like the Arabo-Nubian Shield, where geochemistry and isotopic geochronology of mafic and intermediary complex Ghimbibi-Nedjo, in Ethiopia suggest the opening of oceanic basin between 900-850 Ma (implementation of tholeiitic gabbros) (Woldemichael *et al.*, 2010). There may be an establishment of arc tholeiites associated with a context type arc-back-arc basin, where tholeiitic magmas may erupt. The different fractions display a similar chemical composition with low to high U (25.64 - 1099.2) and Th (4.13-60156) contents and relatively high U/Th (0.14 - 1.75) ratios. This high ratios indicate that, the zircons were crystallized from a mafic magma. Cathodoluminescence images of zircon crystals from amphibolite reveal magmatic oscillatory zoning. Inherited zircons in amphibolites derived from gneiss-amphibole complex (Ca 800.7 Ma). In the Mayo Kebbi region, the wide range of Neoproterozoic sources, evidence of concordant zircon ages at 691 and 800.7 has been recorded. This suggests that Mayo Kebbi basin was filled by sediments, the source of which is mainly reworked Neoproterozoic protoliths and rocks of similar age (ca. 780 Ma) as those recognized in the neighbouring Poli region in Cameroon (Toteu *et al.*, 2006). The rock samples could have been formed as back-arc basalt (Gale and Pearce, 1982; Tarney *et al.*, 1981), and the consensus is therefore that a high proportion of basalt from back-arc basins is transitional in composition between MORB and IAB (Pearce *et al.*, 2006). This may be due to contamination or metasomatism with subduction zone fluids (Gale and Pearce, 1982; Tarney *et al.*, 1981). Tectonic discrimination diagrams using chemical attributes suggest a tholeiitic to calc-alkaline affinity for the mafic intrusive and probably formed in back arc setting. The genesis of the back-arc magmas could be related to suprasubduction of the mantle and/or to the partial melting of a shallow mantle by release of lithostatic pressure (Kerim kocak *et al.*, 2007). The very low TiO<sub>2</sub> content of the amphibolite suggest that the protolith was formed in the Arc system. The high Ca content has been attributed also to the high water of Island arc magma, as suggested by Mamberti *et al.*, 2004; Perfitt *et al.*, 1980 argued that the difference in Ti content is related to early crystallization of Fe-Ti oxides (e.g., magnetite and ilmenite) in IAV, which buffers the Ti concentration. Fe-Ti oxide precipitation may in turn depend on oxygen fugacity. Oxygen fugacity is higher in IAV because of the higher water contents. IAV are enriched in water as well as other volatiles compared to MORB and at least some OIB (e.g., Hawaii) (White WM, 1998).

### The present investigation conducted in southwestern Chad allows us to suggest the following conclusions:

- The LA-ICP-MS zircon dating for the amphibolites yields an age of  $8007 \pm 6.7$  Ma, indicating that the Mayo Kebbi mafic ultramafic rock occurred during Neoproterozoic time.
- The AFM diagram of Mafic and ultramafic intrusions indicate high tholeiitic trend, suggesting that the mafic-ultramafic rocks were crystallized from the same parent magma.
- These rocks show flat and slight pattern, and they are probably derived from a depleted mantle source. All of the amphibolites have very low rare earth element fractionation ( $\text{La/Yb} = 0.41$  to 1.68).
- The geochemical signature of tholeiitic metavolcanic rocks suggests their development in an Island-arc and back-arc setting.
- The representative amphibolites from the previously-defined magmatic basement of Mayo Kebbi region in southwestern Chad yielded zircon U-Pb magmatic ages of ~800.7 Ma. These data are consistent with previous results from the Mayo Kebbi region and

indicate that the igneous complexes were derived from a juvenile Neoproterozoic source.

### Acknowledgments

The authors thank the China Scholarship Council (CSC Program) for its financial support in these researches. The authors are grateful to Ho Liang and Da Wang Guang for their helpful comments on the manuscript. The spot analyses from some sample are not normally distributed, indicating the presence of inherited zircon cores. But the spot for the other samples are normally distributed, indicating the absence of inherited zircon cores. This is consistent with their Cathodoluminescence (CL) images. All these zircons grains exhibit high Th/U ratio suggesting magmatic origin. The geochemical and isotopic data indicate that ultramafics-mafics rock are formed in an arc setting. The geochronological data show that this arc is formed between 800.7 and 691 Ma. These and other data point to major episodic igneous events during the Neoproterozoic for example in South China, Australia and many other parts of the continents (Zhang *et al.*, 2009) like the Arabo-Nubian Shield, where geochemistry and isotopic geochronology of mafic and intermediary complex Ghimbibi-Nedjo, in Ethiopia suggest the opening of oceanic basin between 900-850 Ma (implementation of tholeiitic gabbros) (Woldemichael *et al.*, 2010). There may be an establishment of arc tholeiites associated with a context type arc-back-arc basin, where tholeiitic magmas may erupt.

## REFERENCES

- Abdelsalam, M., Liégeois, J.P., Stern, R.J., 2002. The Saharan metacraton. Journal of African Earth Sciences 34, 119–136.
- Anderson, T., 2002. Correction of common Pb in U-Pb analyses that do not report  $^{204}\text{-Pb}$ . Chemical Geology, 192 (1/2), 59–79.
- Cavosie, A.J., Wilde, S.A., Liu, D., Weiblen, P.W., Valley, J.W., 2004. Internal zoning and U-Th-Pb chemistry of Jack Hills detrital zircons: a mineral record of early Archean to Mesoproterozoic (4348–1576 Ma) magmatism, Precambrian Research 135, 251–279.
- Boynton, W.V., 1984. Geochemistry of the rare earth elements: Meteorite studies. In: Henderson P (ed): Rare Earth Elements Geochemistry. Amsterdam: Elsevier, 63–144.
- Doumng, Jean-C., Poulet, A., Vidal, M., Vicat, J.-P., 2004. Lithostratigraphie des terrains panafricains du Sud du Tchad (région du lac de Léré) et signification géodynamique des formations magmatiques, IGCP second annual Field conference. 5–10<sup>th</sup> January 2004 Garoua, Cameroun, PP.8.
- Doumng, Jean-C., 2006. Géologie des formations Néoproterozoïques du Mayo Kebbi (Sud-Ouest du Tchad). Apport de la Pétrologie et la Géochimie à l'implication sur la géodynamique du Panafrican. THÈSE DE DOCTORAT: UNIVERSITÉ D'ORLÉANS pp. 222.
- Gale, G. H., Pearce, J. A., 1982. Geochemical patterns in Norwegian greenstones. Canadian Journal of Earth Sciences 19, 385–397.
- Guide investisseur minier, 1995. République du Tchad, Ministère des mines, de l'énergie et du pétrole PNUD CHD/91/007, pp. 57.
- Irvine, T.N., Baragar, W.R.A., 1971. A guide to the chemical classification of the common volcanic rocks. Canadian Journal of Earth Sciences 8, 523–548.
- İşcen, M., A.S., Vanderhaeghe, O., Barbey, P., Deloulé, E., 2012. A-type granites from the Pan-African orogenic belt in southwestern Chad constrained using geochemistry, Sr-Nd isotopes and U-Pb geochronology: Lithos, 153, 39–52.
- Liégeois, J.P., Berza, T., Tatu, M., Duchesne, J.C., 1996. The Neoproterozoic Pan-African basement from the Alpine Lower Danubian nappe system (South Carpathians, Romania): Precambrian Research 80, 281–301.
- Kasser, M., 1995. Evolution Précambrienne de la région de Mayo Kebbi (Tchad). Un segment de la chaîne Pan-Africaine. Thèse de doctorat: Muséum National d'Histoire Naturelle, Paris France, pp. 217.
- Kocak, K., Kurt, H., Zedef, V., Ferre, E.C., 2007. Characteristics of the amphibolites from Nigde metamorphics (Central Turkey),

- deduced from whole rock and mineral chemistry. *Geochemical Journal* 41, 241–257.
- Liégeois, J.P., Abdelsalam,M.G., Ennih,N., Ouabadi,A., 2012. Metacraton: Nature, genesis and behavior: *Gondwana Research* 23 (1), 220-237.
- Li YF., Lai, S.C.Qin, J.F., Liu, X., Wang, J., 2007. Geochemical characteristics of Bikou volcanic group and Sr- Nd-Pb isotopic composition: Evidence for breakup event in the north margin of Yangtze plate, Jining era Science in China Series D: Earth Sciences Sci 50, 339-350.
- Ludwig, K., 2003. Isoplot/Ex, version 3.00: a geochronological toolkit for Microsoft Excel Berkeley Geochronology Center Special Publications No. 4.
- Mamberti, M., Lapierre H., Bosch, D., Jaillard, E., Hernandez, J., Polv é, M., 2004. The Early Cretaceous San Juan Plutonic Suite, Ecuador a magma chamber in an oceanic plateau: *Canadian Journal of Earth Sciences* 41, 1237-1258.
- Meschede M., 1986 A method of discriminating between different types of mid-ocean ridge basalts and continental tholeites with the Nb-Zr-Y diagram; *Chemical Geology* 56, 207–218.
- Vrklijan, M., Garašić V., 2004. Different geochemical signatures developed in some basic magmatic rocks of mt. kalnik (North Croatia). *Rud.-geol.-naft. zb* 16. 65-73.
- Pearce, J.A.. 1980. Geochemical evidence for the genesis and eruptive setting of lavas from Tethyan ophiolites [M]. In: Panayiotou A, eds. Proc Intemet Ophiolite Svmp, Cyprus, 1979. Geol Surv Dept. Nicosia. Cv̄nus. p. 261—272.
- Pearce, J. A., Stern, R. J., (2006). Origin of back-arc basin magmas: Trace element and isotope perspectives, Back-Arc Spreading Systems: 63-86.
- Perfit, M. R., Gust, D. A., Bence, A. E., Arculus R. J., Taylor, S. R., 1980. Chemical characteristics of island-arc basalts: implications for mantle sources. *Chemical Geology* 30, 227-256.
- Penaye J., Kroñer A., Toteu Sadrack F., William R., Schmus V., Doummang Jean-C., 2006. Evolution of the Mayo Kebbi region as revealed by zircon dating: An early (ca. 740 Ma) Pan-African magmatic arc in southwestern Chad: *Journal of African Earth Sciences* 44, 530–542.
- Pouclet A., Vidal, M., Doumnang, Jean-C., Vicat, J.-P Tchameni, R., 2006. Neoproterozoic crustal evolution in Southern Chad: Pan-African ocean basin closing, arc accretion and late- to post-orogenic granitic intrusion: *Journal of African Earth Sciences* 44, 543–560.
- Sadrack Félix Toteu, Penaye, J., Deloule,E., Van Schmus,W.R., Tchameni,R., 2006. Diachronous evolution of volcano-sedimentary basins north of the Congo craton: Insights from U-Pb ion microprobe dating of zircons from the Poli, Lom and Yaounde' Groups (Cameroon) *Journal of African Earth Sciences* 44, 428–442.
- Shervais, J.W., (1982). Ti-V plots and the petrogenesis of modern and ophiolitic lavas. *Earth Planet. Sci.Lett* 59, 101–118.
- Tarney, J., Saunders, Matthey, A. D., Wood, D. P., Marsh, D. A., N. G. Marsh,
- Roberts, D., Stegenga, L., 1981. Geochemical aspects of back-arc spreading in the Scotia Sea and western Pacific. *Phil. Trans. R. Soc. London A300*, 605–625.
- Winchester, J.A., Floyd, P.A., 1976. Geochemical magma type discrimination: application to altered and metamorphosed basic igneous rocks. *Earth and Planetary Science Letters* 28, 459–469.
- Woldemichael, B., Kimura, J.I., Dunkley, D., Tani, K. & Ohira, H., 2010. SHRIMP U-Pb zircon geochronology and Sr-Nd isotopic systematic of the Neoproterozoic Ghimbi-Nedjo mafic to intermediate intrusions of Western Ethiopia: a record of passive margin magmatism at 855 Ma? *International Journal of Earth Sciences* 44, 530–542.
- Wood, D. A., 1980. The application of a Th-Hf-Ta diagram to problems of tectonomagmatic classification and to establishing the nature of crustal contamination of basaltic lavas of the British Tertiary volcanic province. *Earth Plan. Sci. Lett* 50, 11–30.
- White, W. M.1998. *Geochemistry of the Solid Earth II*, Chapter 12: The Crust, 512-554.
- Zhang, Z., Zhu, W., Shu, L., Su, J., Zheng, B., 2009. Neoproterozoic Ages of the Kuluk stage Diabase Dyke Swarm in Tarim, Nw China, and Its Relationship to the Breakup of Rodinia *Geological Magazine* 146 (01), 150-154.
- Zhou, J., Wang, X., Qiu, J., Gao J., 2004. Geochemistry of Meso- and Neoproterozoic mafic-ultramafic rocks from northern Guangxi, China: Arc or plume magmatism? *Geochemical Journal* 38, 139 - 152.

\*\*\*\*\*